



Multiparametric Whole Blood Dissection: A One-Shot Comprehensive Picture of the Human Hematopoietic System

Luca Basso-Ricci,^{1†} Serena Scala,^{1†} Raffaella Milani,² Maddalena Migliavacca,^{1,3} Attilio Rovelli,⁴ Maria Ester Bernardo,^{1,3} Fabio Ciceri,⁵ Alessandro Aiuti,^{1,3,6*} Luca Biasco^{1‡*}

¹San Raffaele Telethon Institute for Gene Therapy (SR-TIGET), San Raffaele Scientific Institute, Milan, 20132, Italy

²Cytometry Laboratory, San Raffaele Scientific Institute, Milan, Italy

³San Raffaele Scientific Institute, Pediatric Immunohematology and Bone Marrow Transplantation Unit, Milan, Italy

⁴BMT Unit, Pediatric Department, Milano-Bicocca University, MBBM Foundation, Monza, Italy

⁵San Raffaele Scientific Institute, Hematology and Bone Marrow Transplantation Unit, Milan, Italy

⁶Vita Salute San Raffaele University, Milan, Italy

Received 11 December 2016; Revised 11 April 2017; Accepted 17 May 2017

Grant sponsor: Italian TELETHON foundation (SR-TIGET Core grant C1)

Grant sponsor: European Commission (Advanced Cell-based Therapies for the treatment of Primary Immuno-Deficiency), Grant number: FP7-HEALTH-F5-2010-261387 (CELL-PID)

Grant sponsor: Italian Ministry of Health (New strategies for gene therapy of primary immunodeficiencies using regulated lentiviral vector and gene targeting approaches, NET Program); Grant number: NET-2011-02350069.

Additional Supporting Information may be found in the online version of this article.

• Abstract

Human hematopoiesis is a complex and dynamic system where morphologically and functionally diverse mature cell types are generated and maintained throughout life by bone marrow (BM) Hematopoietic Stem/Progenitor Cells (HSPC). Congenital and acquired hematopoietic disorders are often diagnosed through the detection of aberrant frequency or composition of hematopoietic cell populations. We here describe a novel protocol, called “Whole Blood Dissection” (WBD), capable of analyzing in a single test-tube, hematopoietic progenitors and all major mature cell lineages composing either BM or peripheral blood (PB) through a multiparametric flow-cytometry analysis. WBD allows unambiguously identifying in the same tube up to 23 different blood cell types including HSPC subtypes and all the major myeloid and lymphoid lineage compartments at different stages of maturation, through a combination of 17 surface and 1 viability cell markers. We assessed the efficacy of WBD by analyzing BM and PB samples from adult ($n = 8$) and pediatric ($n = 9$) healthy donors highlighting age-related shift in cell composition. We also tested the capability of WBD on detecting aberrant hematopoietic cell composition in clinical samples of patients with primary immunodeficiency or leukemia unveiling expected and novel hematopoietic unbalances. Overall, WBD allows unambiguously identifying >99% of the cell subpopulations composing a blood sample in a reproducible, standardized, cost-, and time-efficient manner. This tool has a wide range of potential pre-clinical and clinical applications going from the characterization of hematopoietic disorders to the monitoring of hematopoietic reconstitution in patients after transplant or gene therapy. © 2017 The Authors. Cytometry Part A Published by Wiley Periodicals, Inc. on behalf of ISAC.

• Key terms

hematopoiesis; hematopoietic stem cells; flow-cytometry; leukemia; immunodeficiency

HUMAN hematopoiesis is a hierarchically organized system in which distinct cell types with disparate properties and characteristics are continuously generated from primitive hematopoietic progenitors, mainly resident in the bone marrow (BM). Several pathological conditions such as immunodeficiencies and tumors are associated with an altered hematopoiesis with unbalanced frequency of immature vs. mature cell types or aberrant cell phenotypes (1–13). Primary immunodeficiencies (PID) are a heterogeneous group of genetic inherited disorders which affect distinct components of the innate and adaptive immune system, with impairment of their differentiation and/or functions (3,4,6,10,14–17). Although the treatment of choice for the most severe variants of PID patients remains bone marrow transplantation (BMT), over the last decades, gene therapy (GT) based on autologous infusion of gene-corrected hematopoietic stem and progenitor cells (HSPC), has proven, in many cases, to be a safe and efficacious clinical alternative (18–25). Abnormal hematopoiesis can also result from the aberrant expansion of transformed hematopoietic cells.

*Correspondence to: Alessandro Aiuti, SR-TIGET, Scientific Institute San Raffaele, via Olgettina 60, 20132, Milano, Italy. Email: aiuti.alessandro@hsr.it and Luca Biasco, Gene Therapy Program, Dana-Farber/Boston Children's Cancer and Blood Disorders Center; Office Location: SM-1158C, 1 Jimmy Fund Way, Boston, MA 02115. Email: Luca_Biasco@dfci.harvard.edu

[†]LBR and SS contributed equally to this work.

[‡]Current address: Gene Therapy Program, Dana-Farber/Boston Children's Cancer and Blood Disorders Center, Boston, Massachusetts 02115

Published online 13 June 2017 in Wiley Online Library (wileyonlinelibrary.com)

DOI: 10.1002/cyto.a.23148

© 2017 The Authors. Cytometry Part A Published by Wiley Periodicals, Inc. on behalf of ISAC. This is an open access article under the terms of the Creative Commons Attribution-NonCommercial License, which permits use, distribution and reproduction in any medium, provided that the Contribution is properly cited and is not used for commercial purposes.

In case of Acute Lymphoid Leukemia (ALL) and Acute Myeloid Leukemia (AML) the leukemic blasts dominate the BM compartment with profound suppression of other hematopoietic lineages (1,2,11,13,26–28). Leukemic blasts often display aberrant immunophenotypes differing from normal mature cells on the presence of immature-cell surface markers and low/mild CD45 expression (1,2,29,30). Chemo(radio)therapy and BMT from allogeneic donors are the conventional treatments for leukemic patients. Treated individuals remain monitored overtime for the detection of minimal residual disease (MRD) that might evolve in relapse events (31–33).

Human HSPC are commonly exploited for allogeneic and autologous transplantation, including GT as they have high differentiation and proliferation potential, long-term survival capacity and self-renewal ability (18,21,22,24). They are phenotypically characterized by the absence of mature lineage markers (LIN⁻) and by the expression of the CD34 molecule. Through the use CD38, CD90, CD45RA, CD10, CD7 and CD135 markers, seven different HSPC subsets with diverse differentiation and survival potential have been identified (34–37). Various agents are capable of mobilizing the HSPC from the BM niche to the PB, increasing the accessibility and the number of cells available for transplantation (38,39). Under physiological conditions, few HSPC are found in PB of untreated subjects (40–42) and, in absence of pharmacological mobilization, their amount in the periphery is a marker of disease progression and/or of treatment efficacy for several hematopoietic disorders (43–46).

Morphological examination is one of the routine laboratory tests performed for the diagnosis of hematopoietic/immunological disorders, when alterations of the physiological differentiation of hematopoietic cells are suspected (1,29,47). Still, this test requires experienced investigators, it is time consuming, not accurate in quantification and the identification of rare blood cell types through this method could be difficult. Conversely, through the simultaneous measurement of multiple fluorescent antibodies each binding to a specific surface or intracytoplasmatic molecule, flow cytometry provides a highly quantitative and reproducible technique (1,2,30,47–49). To assess the relative frequencies of blood cellular components, cytometric analyses are commonly performed (1,2,48–52) by splitting the available biological sample on different test tubes, each dedicated to the analysis of a restricted group of leukocyte subpopulations through a

limited set of surface markers. As a result, the standard analyses do not allow identifying co-expression of >6–8 independent markers at a time and the relative frequency of all the different blood cell subtypes cannot be concomitantly assessed on the same sample (1,47,51,53). When applied to the study of human HSPC subtypes, cytometric evaluation is generally confined to the CD34⁺ compartment or performed on CD34⁺ cells purified from BM samples through magnetic beads or FACS-sorting (34–37,54). This implies collecting a relatively high amount of cells from the BM as the isolation protocol might lead to the loss of a substantial fraction of the original sample.

Recently, mass spectrometry-based flow cytometry has been developed to increase the resolution of multiparametric analyses allowing studying simultaneously a large number of different cell markers (48,55,56). CyTOF (Time-of-Flight cytometer) mass cytometer is able to combine single cell analysis typical of flow cytometry, with the high resolution and sensitivity of TOF-mass spectrometry (55,56) exploiting heavy metal isotopes conjugated to molecules bind to antibodies. Overcoming some of the existing challenges in flow cytometry, CyTOF has been exploited to characterize diverse populations of immune cells (56). However, the extensive optimization of panel design, the high cost of the instrumentation, the need for specialized personnel and the time required for the analysis limit the application of this promising technology for routine laboratory tests (55).

Addressing these issues, we designed a novel flow cytometry protocol that we called Whole Blood Dissection (WBD), which combines 17 surface markers and 1 viability cell marker accounting for a wide spectrum of hematopoietic lineages. Starting from a limited amount of whole blood (WB), WBD allows analyzing at one time in a single test tube up to 23 different blood cell types composing either BM or PB samples including HSPC subpopulations and all the major cell lineages at different stages of maturations.

MATERIALS AND METHODS

Biological Sample Sources Description

Bone Marrow (BM) and peripheral blood (PB) samples were collected at Ospedale San Raffaele in Milan with approval of the San Raffaele Scientific Institute's Ethics Committee and consent from parents or subjects. Blood was drawn via sterile venipuncture into vacutainers containing K2EDTA

Table 1. List of markers used to identify hematopoietic subtypes in WBD protocol: combination of markers used for the definition of the hematopoietic subpopulations upon WBD

iPMN	CD45+ CD33+ CD66b+ SShigh CD10- and/or CD11c-
PMN	CD45+ CD33+ CD66b+ SShigh CD10+ CD11c+
Monocyte	CD45+ CD33+ CD14+
DC	CD45+ CD33+ CD14- CD11c+
Myeloblast	CD45+ CD33+ CD14- CD11c- CD34-
T Cell	CD45+ CD33- CD66b- CD3+ CD56-
NKt Cell	CD45+ CD33- CD66b- CD3+ CD5&+
NK Cell	CD45+ CD33- CD66b- CD3- CD19- CD56+
B Cell	CD45+ CD33- CD66b- CD3- CD19+ CD10- CD34-
PRE-B	CD45+ CD33- CDG6b- CD3- CD19+ CD10+ CD34-
Pro-B	CD45+ CD33- CD66b- CD3- CD19+ CD10+ CD34+
Pro-lymphocyte	CD45+ CD33- CD66b- CD3- CD19- CD56- CD34- CD71- CD41/61- CD7+ or CD10+
Pro-erythroblast	CD45+ CD33- CD66b- CD3- CD19- CD56- CD34- CD71+
Erythroblast	CD45-CD71+
HSC	CD45+CD14- CD11c- CD3- CD19- CD56- CD34+ CD38- CD90+ CD45RA-
MPP	CD45+CD14- CD11c- CD3- CD19- CD56- CD34+ CD38- CD90- CD45RA-
MLP	CD45+CD14- CD11c- CD3- CD19- CD56- CD34+ CD38- CD90- CD45RA+
ETP	CD45+CD14- CD11c- CD3- CD19- CD56- CD34+ CD38+ CD7+
Pre-B/NK	CD45+CD14- CD11c- CD3- CD19- CD56- CD34+ CD38+ CD7- CD10+ CD45RA+
CMP	CD45+CD14- CD11c- CD3- CD19- CD56- CD34+ CD38+ CD7- CD10- CD135+ CD45RA-
GMP	CD45+CD14- CD11c- CD3- CD19- CD56- CD34+ CD38+ CD7- CD10- CD135+ CD45RA+
MEP	CD45+CD14- CD11c- CD3- CD19- CD56- CD34+ CD38+ CD7- CD10- CD135- CD45RA-

5.4 mg (Becton Dickinson (BD) Vacutainer®; REF no. 8019839). Bone marrow was drawn from the iliac crest with a bone marrow aspiration needle 16G (VIGEO REF no. VV11625/65) in a syringe of 10 ml (BD Emerald™ REF no. 307737) and put into a vacutainer containing K2EDTA 5.4 mg (Becton Dickinson (BD) Vacutainer®; REF no. 8019839).

Whole Blood Dissection Staining

PB and BM aspirate were stained according the protocol described in the “Supporting Information” Section. In brief, after RBC lysis, the samples were labeled with fluorescent antibodies against CD3, CD56, CD14, CD61/41, CD135, CD34, CD45RA (Biolegend) and CD33, CD66b, CD38, CD45, CD90, CD10, CD11c, CD19, CD7, and CD71 (BD Biosciences). The conjugated fluorochromes are reported in Table 1. Titration assays were performed to assess the best antibody concentration. After surface marking, the cells were incubated with PI (Biolegend) to stain dead cells. All samples were acquired through BD LSR-Fortessa (BD Bioscience) cytofluorimeter after Rainbow beads (Spherotech) calibration and raw data were collected through DIVA software (BD Biosciences). The data were subsequently analyzed with FlowJo software Version 9.3.2 (TreeStar) and the graphical output was automatically generated through Prism 6.0c (GraphPad software).

Cell Sorting and Morphological Evaluation

To isolate the different whole blood subpopulations for morphological validation we set up 5 different sorting strategies. Sorting 1 was performed to isolate T, NKt, NK and all CD19+ cells. Sorting 2 was performed to isolate mature B cells, Pre-B, and Pro-B precursors. Sorting 3 was performed to isolate PMN, iPMN, Monocytes and DCs. Sorting 4 was

performed to isolate erythroblasts and Myeloblasts. Sorting 5 was performed to isolate pro-erythroblasts and lymphoid-committed progenitors (Pro-Lymphocytes). The list of the markers used in each sorting panel is shown on Figure 2A. We performed our morphological validation on BM samples from HD. The samples were prepared according to the steps 1–12 described in the WBD protocol, except for sorting 3 as monocytes are very sensitive to manipulations and their isolation required a different protocol. In brief, after the lysis step, we performed two rounds of platelets elimination through centrifugation at 160 rcf RT for 10 min. Additionally, in order to keep the monocytes alive, we used the WS buffer instead of PBS-FACS for all the steps and we worked on ice (See also Supporting Information). All the samples were FACS-purified by MoFlo-XDP cell sorter (Beckman Coulter). The cells were immobilized immediately after sorting onto glass microscope slides by cytospin (Cytospin3, Shandon) centrifugation and then colored with May-Grunwald/Giemsa (Sigma) staining. Images were collected using Axioskop40 microscope and AxioCam MRc5 camera and analyzed through Axiovision 4.8 Software (Zeiss). Morphological evaluation was performed in blind by a specialized hematologist.

Statistical Analysis

Statistical analyses were performed with Prism 6.0c (GraphPad software). Data are shown as mean ± SEM, unless otherwise specified. Tables displaying hematopoietic cell subtype frequencies report mean ± S.D. Analytical tests for statistical significance among groups employed Mann-Whitney test (*P* values are specified in each figure legend).

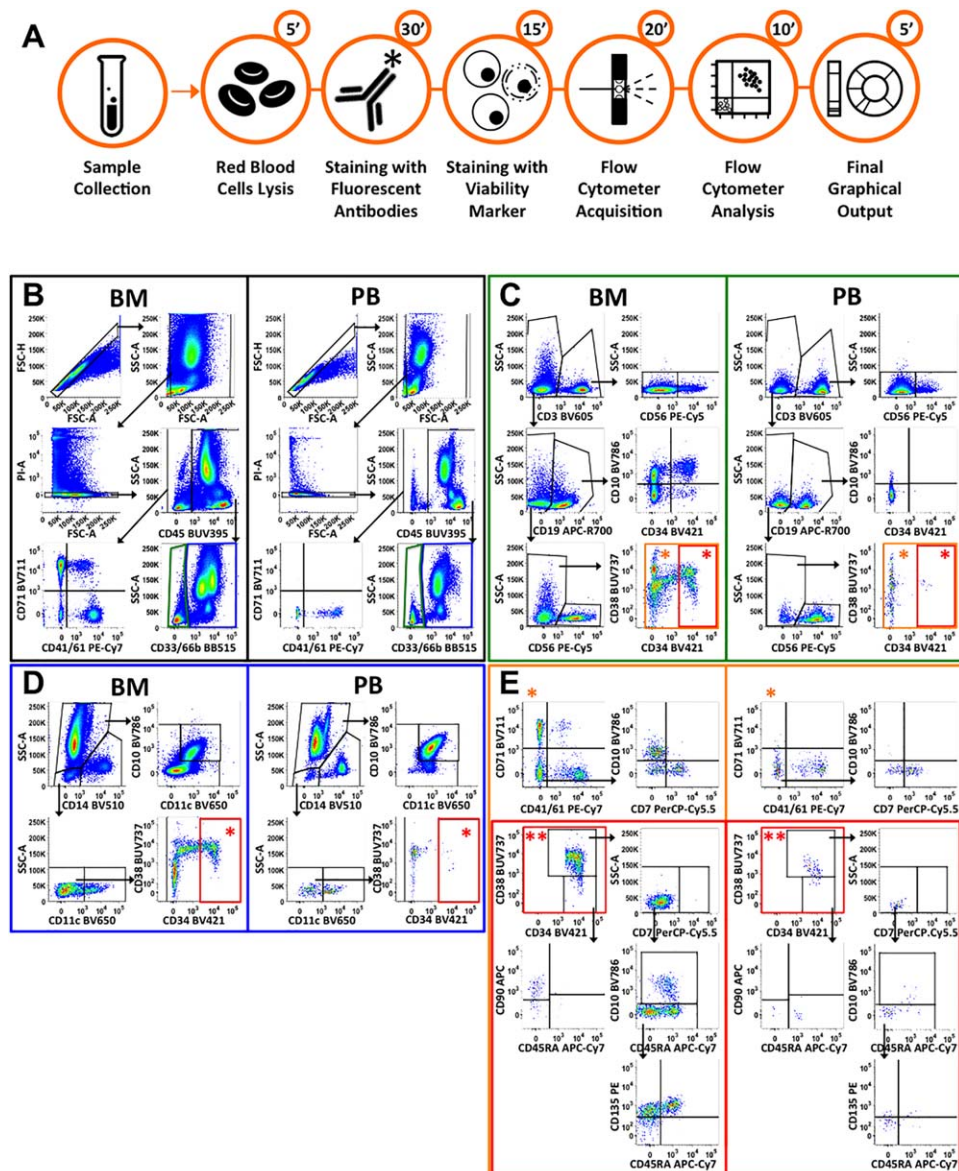


Figure 1. WBD protocol workflow and gating strategy: **(A)** WBD protocol workflow. After BM or PB sampling, the red blood cells are lysed and the samples are stained with the fluorescent antibodies against the WBD markers. The following steps comprise: incubation with Propidium Iodide (PI) to discriminate live and dead cells, acquisition to LSR-Fortessa (BD Bioscience), data analyses and graphical sample composition representation. The numbers in the smaller circles indicate the minutes required for performing each step: once setup, the final WBD results are available in <1.5 h from the arrival of the samples. See Supporting Information for the detailed description of the protocol **(B–E)** Gating strategy for characterization of healthy donor (HD) bone marrow (BM, left side of the colored frames) and peripheral blood (PB, right side of the colored frames). **(B)**, black frame: after physical parameters, live/dead and pan-leukocyte CD45 marker expression discrimination, the gating strategy identifies myeloid (blue gate) and not-myeloid cells (green gate). **(D)**, blue frame: Myeloid cell subtypes and myeloid-committed CD34+ cells (red gate and asterisk). **(C)**, green frame: gating strategy for not-myeloid cells identifies lymphoid and Lineage negative (LIN-, orange gate) cells. Lin- cells are separated on the basis of CD34 expression as LIN-CD34- (orange asterisk) and LIN-CD34+ (red gate and asterisk) cells. **(E)**, orange frame: LIN-CD34- subtypes (orange asterisk); red frame: HSPC subpopulations analyzed from the merge of myeloid-committed CD34+ (from panel **D**) and LIN-CD34+ (from panel **C**) cells (double red asterisks). [Color figure can be viewed at wileyonlinelibrary.com]

RESULTS

Technical Set up of the WBD Protocol

The WBD workflow comprises a step of red blood cells (RBC) lysis on WB samples followed by the immunostaining for surface and viability markers, the FACS acquisition and data analysis (Fig. 1A). The complete protocol is described in

details in the Supporting Information section. For the original setup we identified the most informative surface molecules capable of unambiguously discriminating cell subpopulations and the optimal fluorochrome-marker combination to avoid co-expression of markers conjugated to fluorochromes with major spectral overlap. In order to reduce at minimum artifacts due to the changes in morphology and surface antibody

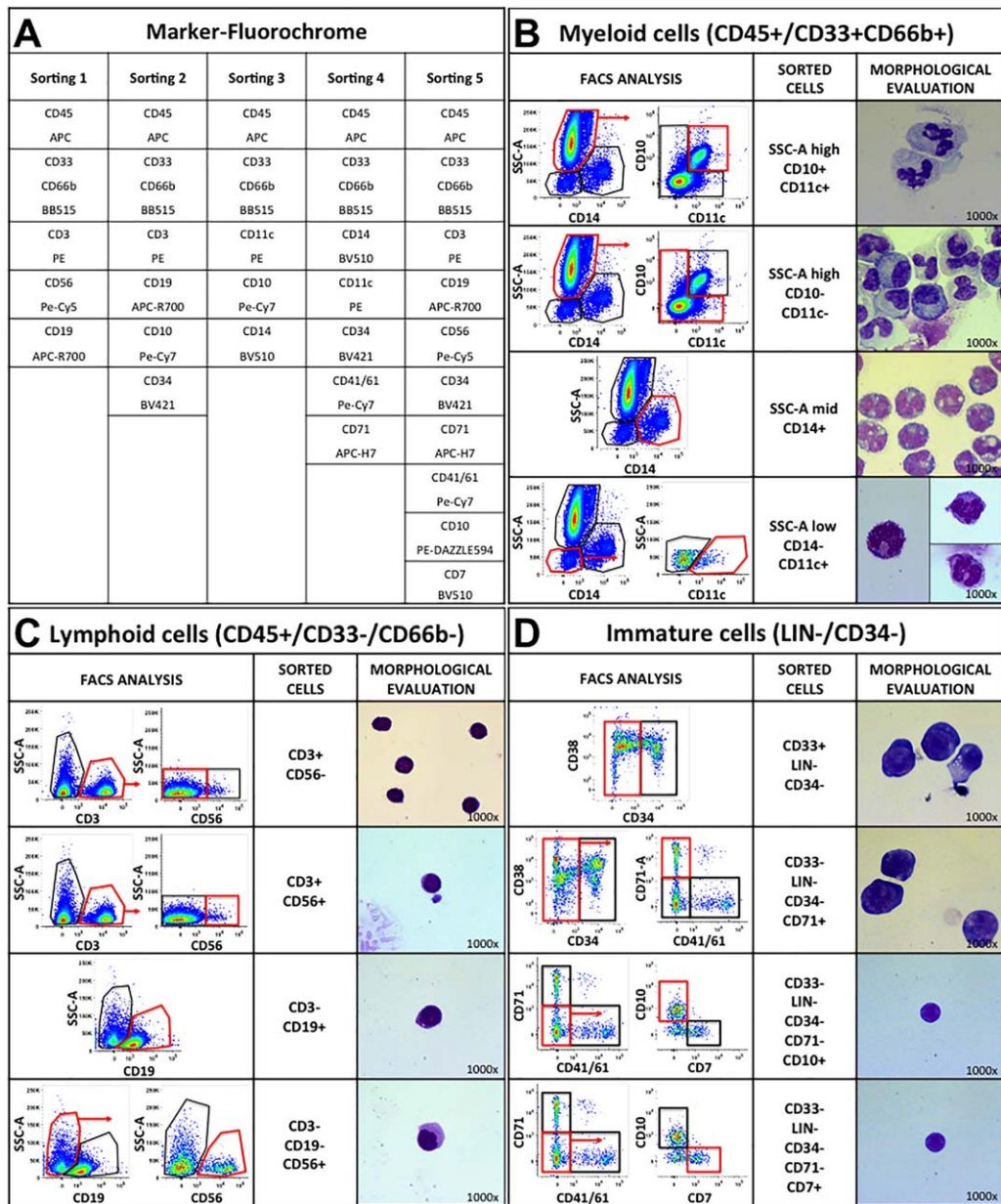


Figure 2. Morphological validation of WBD protocol: tables showing the sorting strategies and the resulting morphology of myeloid (B), lymphoid (C) and immature (D) cell subtypes isolated from bone marrow of healthy donors. Cells were sorted according to the markers listed in Table A and on the basis of the gating strategy described in “Figures 1B–1E.” For each compartment, the dot plots show the physical parameters (left plot) and the markers (right plot) used to identify and sort the different subpopulations. The pictures on the right show the observed morphology of the isolated cells (May-Grunwald-Giemsa staining; magnification reported on the bottom right corner of each picture). [Color figure can be viewed at wileyonlinelibrary.com]

binding properties of pre-apoptotic and apoptotic cells we included in our staining a viability marker (PI). After viability selection, we excluded mature RBC and non-hematopoietic cells through the expression of CD45 pan-leukocyte marker.

To identify HSPC subtypes, we made use of the panel of markers described in Doulatov et al. (34). In particular, we exploited CD34, CD38, CD45RA, CD90, CD7, CD10 and CD135 markers to classify primitive and committed progenitors. Among the primitive subsets (LIN-/CD34+/CD38–) we

identified hematopoietic stem cells (HSC), multipotent progenitors (MPP) and multi-lymphoid progenitors (MLP). The committed progenitors (LIN-/CD34+/CD38+) were dissected into early T progenitors (ETP), B and NK cell precursors (Pre-B/NK), common myeloid progenitors (CMP), granulocyte-monocyte progenitors (GMP) and megakaryo-erythroid progenitors (MEP). We then selected additional antibodies for dissecting LIN+ cell subsets. The CD33 marker is expressed on the vast majority of myeloid cells while CD66b

is an adhesion molecule involved in chemotaxis expressed exclusively on Polymorphonucleated cells (PMN) (1,57). Thus we evaluated the concomitant or alternative expression (and/or expression, from now on referred to as CD33 + CD66b+) of CD33 and CD66b markers, here conjugated with the same fluorochrome, for identifying myeloid (CD33 + CD66b+) and nonmyeloid (CD33-/CD66b-) cells. We then further dissected myeloid subsets through their morphological complexity parameter (SSC-A) and through the presence or absence of CD14 and CD11c surface molecules. CD14 is a pan-monocytes marker, while CD11c is present on circulating mature dendritic cells and their precursors (DC). To discriminate the major lymphocyte subsets we used CD3, CD19 and CD56 surface markers. CD3 antigen is a classical marker of mature T cells. Mature B lymphocytes and different state of B-cell maturation can be identified through their expression of the pan-B CD19 marker in combination with the CD34 and CD10 markers (1,57). CD3-/CD19-/CD56+ lymphocytes are Natural Killer (NK) cells, while the co-expression of CD56 and CD3 tags the so-called Natural Killer T (NKt) cells, a population with a restricted TCR repertoire mainly involved in anti-tumor response (58,59). For the identification of platelets (PLTs), we selected a cocktail of antibodies (anti-CD41/CD61) capable of recognizing both mature (CD45-) and immature (CD45+) platelets. Four different stages of maturation have been described for erythroid cells on the basis of the expression of CD34, CD45, CD71 and CD235a (1,60). In particular, CD71 transferrin receptor is expressed in the two intermediate steps of RBC development before the nucleus extrusion. Importantly, CD71+ immature erythroid cells are not lost during the RBC lysis step. The complete list of the hematopoietic subpopulations identifiable through WBD is reported in Table 1.

The high number of markers in WBD protocol required an accurate study of marker co-expression and fluorochrome emission spectra overlap to reduce at minimum technical artifacts (61). The complete list of the markers and the fluorochromes necessary for performing the WBD protocol is reported in Supporting Information Table S1. In order to exclude false positive events, due to auto-fluorescence and to the complex compensation required to avoid signal spill over, we performed Fluorescent-Minus-One (FMO) controls for all the WBD markers (Supporting Information Fig. S1). All the gates were then set on the basis of the FMO control samples. Finally, Rainbow beads (61) calibration was performed before each acquisition for achieving comparable instrument setup among different experiments.

Characterizing BM and PB from Healthy Donors through WBD

To test the efficiency of WBD on successfully identifying blood cell subtypes and on reproducibly assessing and discriminating their contribution in human BM and PB, we analyzed 4 BM and 4 PB WB samples from 8 adult (Ad) healthy donors (HD) (Figs. 1B–1E, Supporting Information Fig. S2 and Table S2). In the BM samples the CD45+ fraction contained cell subtypes with more diversified levels of CD45

expression as compared to the PB samples where the vast majority of the cells is CD45^{high} due to their mature differentiation state. In the CD45- fraction of the BM we identified a substantial number of CD71+ erythroblasts (on average 82.4% of CD45- cells), which conversely were almost undetectable in the PB ($P < 0.05$ Mann-Whitney test, Supporting Information Table S2). The CD45+ cells were divided in myeloid (CD45+/CD33 + CD66b+) and nonmyeloid (CD45+/CD33-/CD66b-) populations.

Within the myeloid compartment we distinguished monocytes (SSC-A^{mid}/CD14+) and granulocytes (SSC-A^{high}/CD14-). We then further dissected granulocytes in two populations with different degree of maturation: mature PMN (CD10+/CD11c+) and Immature PMN (iPMN; CD10- and/or CD11c-). In the SSC-A^{low}/CD14- fraction we identified DC through the expression of CD11c while the negative events were divided into myeloid precursors (Myeloblast; CD34-) and myeloid-committed progenitors (CD34+) (Table 1). As expected, we found a higher relative contribution of iPMN and myeloblasts in the BM with respect to PB samples (on average on CD45+ cells, iPMN: 42,4% in BM vs.1,7% in PB, $P < 0,05$; Myeloblasts: 0,9% in BM vs. 0.4% in PB, $P < 0.05$; Mann-Whitney test, Supporting Information Table S2).

Within the nonmyeloid compartment we discriminated T (CD3+/CD56-), NKt (CD3+/CD56+), B (mature: CD19+/CD10-/CD34-; Pre-B: CD19+/CD10+/CD34- and Pro-B: CD19+/CD10+/CD34+), NK (CD3-/CD19-/CD56+) cells and LIN-CD34+ cells (Table 1). We observed that mature T and NKt lymphocytes were significantly more abundant in PB than in BM samples (on average on total CD45+ cells, T cells: 36,2% in PB vs. 14,3% in BM $P < 0.05$; NKt cells: 2% in PB and 0,5% in BM $P < 0.05$; Mann-Whitney test; Supporting Information Table S2). Moreover, in accordance with what expected from the biology of B cell differentiation, we could identify, specifically and only in the BM samples, immature B cells (on average on lymphoid cells, Pre-B 17% and Pro-B 2.8%; Supporting Information Figs. S2C and S2D and Table S2).

Among CD45+/LIN-/CD34- cells we distinguished Pro-erythroblasts (CD71+), immature platelets (CD41/61+) and in the CD71- and CD41/61- compartment we identified two lymphoid-committed subsets (CD10+ or CD7+) (Table 1). As expected, we observed a higher frequency of immature LIN- cells in BM with respect to PB samples (on average on CD45+ cells 2,5% in BM vs.0,2% in PB; $P < 0,05$ Mann-Whitney test; Supporting Information Fig. S2A and Table S2). Interestingly, Pro-erythroblasts were found only in the BM samples (on average on CD45 + LIN- cells: 21.2% in BM vs. 2.1% in PB; $P < 0.05$ Mann-Whitney test; Supporting Information Fig. S2E and Table S2).

We then pooled CD45+/LIN-/CD34+ and CD45+/CD33 + CD66b+/CD34+ populations to analyze the entire HSPC compartment. We identified the most primitive subsets as HSC (CD90+/CD45RA-), MPP (CD90-/CD45RA-) and MLP (CD45RA+). Committed progenitors could be divided into ETP (CD7+), Pre-B/NK (CD7-/CD10), CMP (CD7-/CD10-/CD135+/CD45RA-), GMP (CD7-/CD10-/CD135+/

CD45RA+) and MEP (CD7-/CD10-/CD135-/CD45RA-) (Table 1). Importantly, through WBD we could detect circulating HSPC in PB although at lower level with respect to their BM counterpart, on average 18,4% (PB) and 57,9% (BM) of CD45+/LIN- cells (BM vs. PB $P < 0.05$ Mann-Whitney test, Supporting Information Table S2). Overall, with WBD we were able to univocally classify 23 different subpopulations covering on average the 99.7% of BM and the 99,8% of PB samples. The complete list of BM and PB cell population frequencies and comparative statistical test results are reported on Supporting Information Table S2.

Validating WBD Protocol through Morphological Assays

To assess whether the WBD was properly identifying each cell subtype, we performed five independent FACS sorting on BM samples from HD following the same gating strategy used in the WBD protocol. We then analyzed the morphology of sorted cells in blind tests to verify that it was matching their original phenotypic categorization through WBD (Figs. 2B–2D). The list of markers used for the 5 FACS sorting is reported in Figure 2A. As shown in Figures 2B and 2C, we were able to confirm that the evaluation of the morphology of all sorted myeloid and lymphoid lineages matched the results of the phenotypic characterization performed through our WBD protocol. Notably, the morphological validation of WBD allowed characterizing cell subtypes yet poorly described. Indeed, through WBD we could identify two additional blood cell subpopulations defined as CD45+/CD33–CD66b–/LIN–/CD34–/CD71–/CD10+ and CD45+/CD33–CD66b–/LIN–/CD34–/CD71–/CD7+ phenotype. We speculated that these subsets should have belonged to the lymphoid compartment due to the presence of CD10 and CD7 markers on their surface. Upon morphological evaluation we indeed confirmed that these cells displayed a lymphoid-like appearance being small round cells with a thin rim of cytoplasm (Fig. 2D). Our analysis showed also that, although having a univocal phenotypic definition (Table 1), the iPMN compartment seems actually composed by a morphologically mixed population of immature granulocytes at different stages of differentiation (Fig. 2B).

Testing WBD Protocol on WB Samples from Pediatric Healthy Donors and Patients Affected by PID

To investigate the efficacy of our protocol on detecting aberrant hematopoietic cell composition in patients with hematological disorders, we performed the WBD staining on 22 individuals affected by different diseases, comprising immunodeficiencies and hematological tumors (Supporting Information Table S3). Given that the age of an individual physiologically affects the composition of hematopoietic population, we analyzed BM samples from five pediatric (Ped) HD in addition to our cohort of Ad HD in order to obtain age-matched reference datasets for comparative analyses on pediatric patients. We then applied the WBD protocol on BM samples collected from four pediatric Adenosine Deaminase (ADA)-deficient severe combined immunodeficient (SCID) patients under enzyme replacement therapy and 6 Wiskott-

Aldrich Syndrome (WAS) affected individuals (3 pediatric and 3 adult). These are two PID, whose defects were well characterized in previous studies (4–7,9,16,17,62), comprising altered or partially impaired hematopoiesis. The WBD protocol was able to detect the reduction of the lymphoid compartment and the unbalanced composition of B cell compartment in both PID. In particular, through WBD, in pediatric ADA-SCID patients we could observe abnormal population frequencies in line with the characteristic block in B cell maturation. These patients displayed a higher content of immature B cells with respect to age-matched HD (5) (79.5% vs. 53.9% of PreB cells in ADA-SCID and Ped HD respectively. $P < 0.05$ Mann-Whitney test; Fig. 3C and Supporting Information Fig. S3D and S3E; Table 2) and lower frequencies of mature B cells when calculated on CD19+ cells, on total lymphocytes and on CD45+ cells. In our mixed adult and pediatric WAS patients population, our protocol highlighted the expected lower frequency of the CD19+ lymphocytes (4.6% vs. 12.6% CD19+ cells on total CD45+ cells, $P < 0.01$ Mann-Whitney test) and of the immature Pre-B cell subset within the lymphoid compartment (6.9% vs. 23.5% on total lymphoid cells, $P < 0.01$ Mann-Whitney test; Fig. 3C, Supporting Information Figs. S3D and S3E; Table 2), as compared to the HD group (Ad + Ped) (7,17). Importantly, as WBD allows concomitantly analyzing all major blood cell populations, we were able to retrieve novel information on the BM of PID patients. We could unveil a relative higher percentage of monocytes (7.3% vs. 3.3% on total CD45+ cells; $P < 0.001$ Mann-Whitney test) and NK cells (20.2% vs. 7% on total lymphoid cells; $P < 0.05$ Mann-Whitney test) (Fig. 3C, Supporting Information Figs. S3C and S3D; Table 2) and a reduced HSPC content (0.6% vs. 1.3% on total CD45+ cells; $P < 0.001$ Mann-Whitney test; Fig. 3C, Supporting Information Fig. S3A and Table 2) in our cohort of WAS subjects with respect to HD, while in ADA-SCID patients we found a significant decrease of primitive CD34 + CD38– HSPC compartment with respect to Ped HD (2% vs. 6.9% of CD34 + CD38– cells on HSPC in ADA-SCID and Ped HD respectively; $P < 0.05$ Mann-Whitney test; Fig. 3C, Supporting Information Fig. S3G and Table 2). As controls individuals with a non-hematological disease, we analyzed the BM composition of four pre-symptomatic Metachromatic Leuko-dystrophy (MLD) patients. MLD is an inherited lysosomal storage disease where pre-symptomatic individuals do not display hematopoietic alterations (63,64). As reported in Figure 3D and Supporting Information Figure S3, MLD patients have a blood cell composition similar to Ped HD, with only a slightly higher contribution of CD19+ lymphocytes probably due to the very young age of these individuals (17.6% in MLD vs. 13.4% in Ped HD of CD19+ cells on CD45+ cells; Table 2).

Analyzing Acute Myeloid and Lymphoid Leukemia Samples with WBD

In order to provide a qualitative assessment on the capability of WBD technology to detect unbalances in hematological tumors, we tested the efficacy of our protocol on BM samples from patients with ALL ($n = 1$) and AML ($n = 6$)

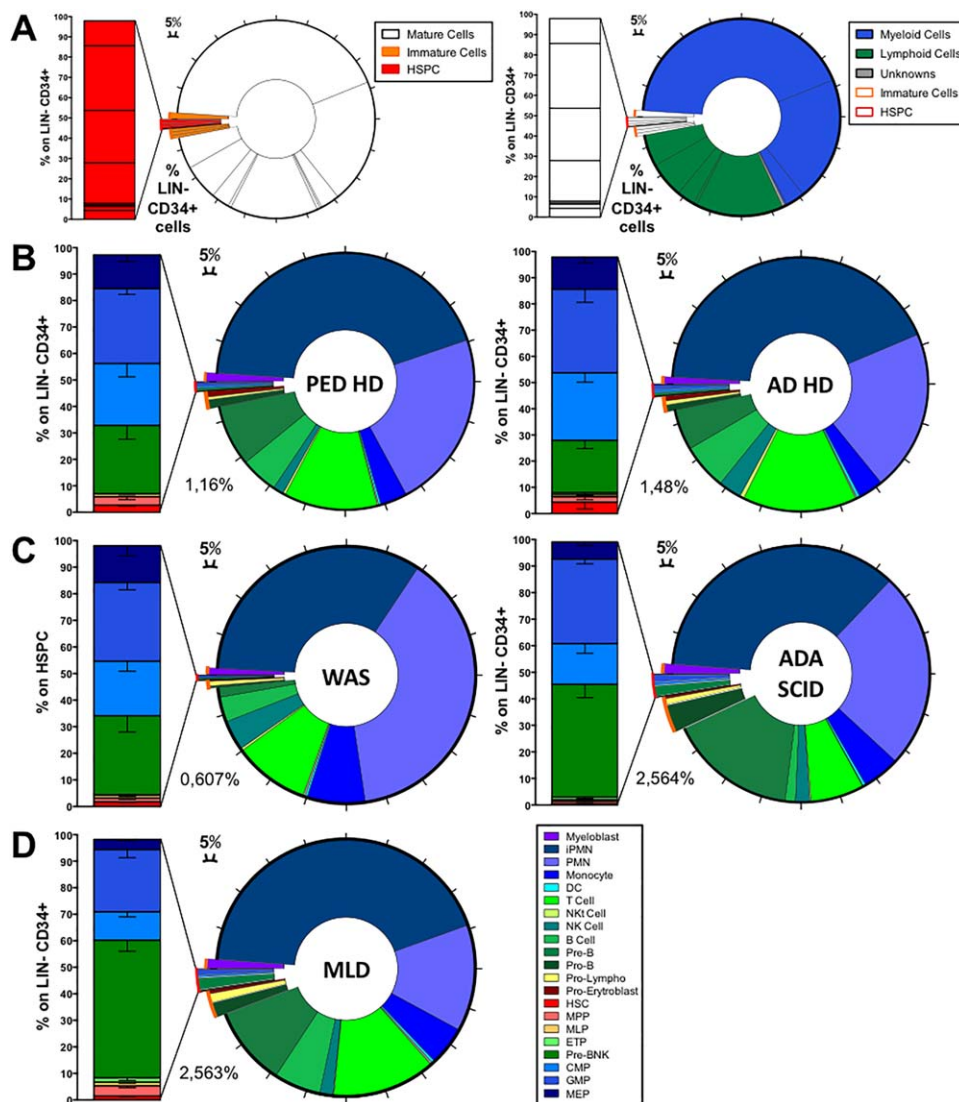


Figure 3. WBD analyses of BM samples from healthy donors and patients: (A) Scheme describing the graphical representation of the CD45⁺ cell composition through WBD protocol. The ring chart shows frequencies of hematopoietic subpopulations on total CD45⁺ cells. Ticks on the circumference of the circular plot were added for a best visual estimation of the relative contribution of the different hematopoietic subtypes (distance between two ticks = 5%). The left panel highlights the immature subpopulations: the “less-exploded” orange section shows immature cells (LIN-CD34⁻ and Pro-B cells) while the “more-exploded” red section shows the frequencies of LIN-CD34⁺ (HSPC) subpopulations on total CD45⁺ cells. The stacked bar graph on the left of the ring chart is a zoom on the frequency of the different HSPC subtypes within the LIN-CD34⁺ compartment. The percentage reported on each graph displays the relative frequency of the LIN-CD34⁺ cells on total CD45⁺ cells. On the right panel, the section of the ring chart highlighted with a bold black outer ring displays the fractions of LIN + CD34⁻ cells divided in myeloid (scale of blues) and lymphoid (scale of greens) subtypes. (B–D) Averages of BM subpopulations’ frequencies in pediatric (B left panel, $n = 5$) and adult (B right panel, $n = 4$) healthy donors (HD) in comparison with WAS (C left panel, $n = 6$), ADA-SCID (C right panel, $n = 4$) patients and MLD (D, $n = 4$) affected individuals. (Ad = adult; Ped = pediatric; WAS = Wiskott-Aldrich Syndrome; ADA-SCID = Adenosine Deaminase-deficient Severe Combined Immuno-deficiency; MLD = Metachromatic Leuko-dystrophy). [Color figure can be viewed at wileyonlinelibrary.com]

(Fig. 4 and Table 2). We analyzed 4 BM samples from patients at diagnosis/relapse, where the expanded clones accounted for the 80–90% of the analyzed materials, and 3 BM samples from patients after chemotherapy, in which only a residual fraction of the aberrant clone was detectable. As shown in Figure 4, through WBD we detected abnormal compositions of hematopoietic compartment and the presence of immature blasts displaying low levels of CD45 marker in all the BM

samples analyzed. Analyzing the expression of CD33 in combination with CD34 marker we could discriminate between myeloid and lymphoid leukemia according to the accumulation of blasts bearing myeloid (Supporting Information Fig. S4B and S4C) or lymphoid (Supporting Information Fig. S4D) markers. Indeed, while in the HD we could discriminate the two major branches of hematopoietic differentiation (Supporting Information Fig. S4A, immature not-myeloid-biased

Table 2. Frequencies of bone marrow subpopulations in healthy donors and patients on total CD45+ cells and on specific compartments: average percentage ± Standard Deviations of BM hematopoietic cells in adult and pediatric healthy donors and in MLD, WAS, and ADA-SCID affected individuals

	ADHD N=4	PED HD N=5	MLD N=4	VERSUS PED HD	WAS N=6	VERSUS HD	ADA-SCID N=4	VERSUS PED HD
% on CD45-								
Erythroblast	82.4 ± 8.7	85.61 ± 2.4	58.1 ± 7.9	*	45.7 ± 36.4	*	60 ± 30.2	ns
% on CD45+								
Myeloid	67 ± 7.6	70.3 ± 8	62.6 ± 3.8	Ns	79.8 ± 7.9	*	65.9 ± 12.9	ns
iPMN	42.4 ± 7.2	43.4 ± 10.1	42.9 ± 5	Ns	33.3 ± 10.5	ns	35.5 ± 10.5	ns
PMN	20.3 ± 2.8	22.2 ± 3.2	13.3 ± 2.2	*	38.1 ± 14.1	*	24.2 ± 13.3	ns
Monocyte	3.1 ± 1.1	3.4 ± 0.8	4.9 ± 2	Ns	7.3 ± 2.3	***	4.7 ± 2.2	ns
DC	0.3 ± 0.1	0.2 ± 0.1	0.3 ± 0.1	Ns	0.3 ± 0.2	ns	0.4 ± 0.1	ns
Myeloblast	0.9 ± 0.1	1 ± 0.3	1.2 ± 0.4	Ns	0.9 ± 0.4	ns	1.2 ± 0.5	ns
Lymphoid	29.3 ± 6.7	26.7 ± 7.9	32.3 ± 4.6	Ns	18.1 ± 7.2	*	26.73 ± 7.9	ns
T Cell	14.3 ± 3.5	11.7 ± 5.8	12.9 ± 3.8	Ns	9.4 ± 4.7	ns	6.7 ± 5.3	ns
NKt Cell	0.5 ± 0.4	0.3 ± 0.2	0.1	*	0.3 ± 0.4	ns	0.2 ± 0.3	ns
NK Cell	2.9 ± 1.6	1.3 ± 0.7	1.7 ± 0.5	Ns	3.7 ± 3.4	ns	1.8 ± 1.7	ns
CD19+ Cell	11.6 ± 4.5	13.4 ± 4.5	17.6 ± 2.1	Ns	4.6 ± 2.3	**	20.5 ± 14.2	ns
B Cell	5.7 ± 2.6	4.7 ± 1.4	5.9 ± 1.9	Ns	3.1 ± 1.5	ns	1.3 ± 1.3	*
Pre-B	5.1 ± 1.9	7.6 ± 3.7	9.9 ± 2.7	Ns	1.2 ± 1	ns	15.8 ± 10.5	ns
Pro-B	0.8 ± 0.5	1.1 ± 0.6	1.8 ± 0.8	Ns	0.3 ± 0.2	**	3.3 ± 3	ns
Immature cell	2.5 ± 0.7	2.1 ± 0.3	3.9 ± 1.6	Ns	1.3 ± 0.7	*	3.5 ± 2.9	ns
Pro-lymphocyte	0.5 ± 0.2	0.3 ± 0.1	1.1 ± 0.9	Ns	0.6 ± 0.4	ns	0.7 ± 0.4	ns
Pro-erythroblast	0.5 ± 0.2	0.7 ± 0.2	0.3 ± 0.1	Ns	0.1 ± 0.1	***	0.3 ± 0.3	ns
HSPC	1.5 ± 0.6	1.2 ± 0.2	2.6 ± 1.0	*	0.6 ± 0.4	***	2.6 ± 2.8	ns
CD38-	0.14 ± 0.18	0.08 ± 0.03	0.16 ± 0.03	Ns	0.03 ± 0.03	*	0.04 ± 0.03	ns
CD38+	1.32 ± 0.41	1.05 ± 0.17	2.36 ± 0.92	*	0.56 ± 0.31	ns	2.49 ± 2.75	ns
% on myeloid (CD45+CD33+CD66b+LIN+)								
iPMN	63 ± 5.8	61.1 ± 9.2	68.4 ± 4.3	ns	42.3 ± 14.4	**	54 ± 13.5	ns
PMN	30.5 ± 4.3	32.1 ± 7.3	21.3 ± 4.2	*	47.1 ± 15.4	ns	35.6 ± 14.7	ns
Monocyte	4.7 ± 1.6	4.9 ± 1.5	7.9 ± 3.4	ns	9.1 ± 2.7	**	7.8 ± 5.2	ns
DC	0.5 ± 0.2	0.4 ± 0.2	0.5 ± 0.2	ns	0.3 ± 0.3	ns	0.6 ± 0.3	ns
Myeloblast	1.3 ± 0.1	1.5 ± 0.4	1.9 ± 0.6	ns	1.1 ± 0.6	ns	2 ± 1.2	ns
% on lymphoid (CD45+CD33- CD66b- Lin+)								
T Cell	49.6 ± 12.1	43.3 ± 12.4	39.5 ± 7.4	ns	52.8 ± 16.8	ns	29.4 ± 27.5	ns
NKt Cell	2 ± 1.4	1.2 ± 0.4	0.3 ± 0.1	*	1.5 ± 1.2	ns	0.7 ± 1.3	ns
NK Cell	9.4 ± 3.7	5 ± 2	5.2 ± 1.7	ns	20.2 ± 16.1	*	5.7 ± 3.8	ns
CD19+Cell	50.5 ± 14.5	39 ± 11.5	55 ± 8	ns	25.5 ± 7.7	**	64.2 ± 28.5	ns
B Cell	18.8 ± 4.7	18.1 ± 5.5	17.9 ± 3.5	ns	17.1 ± 6.4	ns	4 ± 2.4	*
Pre-B	17.4 ± 6.4	28.5 ± 14	31.5 ± 11.7	ns	6.9 ± 4.6	**	50.1 ± 20	ns
Pro-B	2.8 ± 1.8	3.9 ± 2	5.6 ± 2.3	ns	1.5 ± 1.3	*	10.2 ± 8.3	ns
% on CD19+ cells (CD45+CD33-CD66b-CD19+)								
B Cell	49 ± 7.4	38.5 ± 17	33.5 ± 9.9	ns	69.4 ± 22.6	*	7 ± 3.7	*
Pre-B	44.3 ± 5.4	53.9 ± 15	56 ± 11.6	ns	25.1 ± 17.5	*	79.5 ± 4.4	*
Pro-B	6.7 ± 2.4	7.6 ± 2.2	10.4 ± 4.8	ns	5.6 ± 5.3	ns	13.6 ± 7.4	ns
% on immature cell (CD45+Lin-)								
Pro-lymphocyte	20.9 ± 7.7	15.4 ± 5.4	24 ± 13.6	ns	38.5 ± 15.2	**	28 ± 19.6	ns
Pro-erythroblast	21.2 ± 6.8	30.9 ± 7.2	9.8 ± 5	*	16.8 ± 18	ns	8.6 ± 2.7	*
HSPC	57.9 ± 7.7	53.7 ± 6.2	66.2 ± 13.5	ns	44.8 ± 13.5	ns	63.3 ± 20	ns
% on HSPC (CD45+Lin-CD34+)								
CD38-	7.3 ± 7.1	6.9 ± 2.3	6.7 ± 2	ns	4.2 ± 1.8	ns	2 ± 1.5	*
HSC	4.3 ± 5	2.7 ± 0.9	1.4 ± 0.7	ns	1.7 ± 0.6	ns	0.5 ± 0.3	*
MPP	2.1 ± 2.4	3.1 ± 2.5	3.9 ± 1.4	ns	1.4 ± 1.1	ns	0.9 ± 0.9	ns
MLP	0.8 ± 0.7	1.1 ± 0.8	1.4 ± 0.8	ns	1.1 ± 1	ns	0.6 ± 0.5	ns
CD38+	90.6 ± 6.3	90.3 ± 6.3	91.5 ± 2.9	ns	93.8 ± 3.6	ns	97 ± 0.9	*

TABLE 2. Continued

	ADHD N = 4	PED HD N = 5	MLD N = 4	VERSUS PED HD	WAS N = 6	VERSUS HD	ADA-SCID N = 4	VERSUS PED HD
ETP	0.7 ± 1.1	0.2 ± 0.1	1.7 ± 1.9	ns	0.2 ± 0.3	ns	1 ± 1.2	ns
Pre-B/NK	20 ± 6.2	25.7 ± 11.7	51.9 ± 8.3	*	29.7 ± 14.9	ns	42.4 ± 9.9	ns
CMP	25.8 ± 7	23.4 ± 11.3	10.7 ± 3.9	ns	20.5 ± 9.2	ns	15.4 ± 7.3	ns
GMP	31.9 ± 9.9	28.3 ± 5	23.5 ± 6.1	ns	29.6 ± 6.7	ns	31.8 ± 3.6	ns
MEP	12.3 ± 4.4	12.7 ± 5.5	3.8 ± 0.7	*	13.8 ± 9.4	ns	6.4 ± 2.4	ns

Mann-Whitney test was performed to evaluate statistical significance of the difference reported between patients and age-matched HD. Since WAS group is composed by both pediatric and adult individuals we tested statistical significance with respect to Ad ± Ped HD pooled group (* = $P < 0.05$; ** = $P < 0.01$; *** = $P < 0.001$; WAS: Wiskott-Aldrich Syndrome, ADA-SCID: Adenosine Deaminase-deficient Severe Combined Immunodeficiency; MLD: Metachromatic Leuko-dystrophy).

[Q1] and immature myeloid-biased [Q2] progenitors, mature not-myeloid cells [Q3] and mature myeloid cells [Q4]) in the acute leukemic samples we observed a skewing toward a single differentiation pathway and an accumulation of cells at a specific stage of maturation. Furthermore, given the high number of markers concomitantly detectable through WBD, we could now assess the level of differentiation of the aberrant leukemic clones. In particular, we observed that AML-1 and AML-4 showed an accumulation of a less differentiated “GMP-like” population while AML-2 and AML-3 displayed more mature “myeloblast-like” phenotypes (Fig. 4B). Furthermore, to evaluate the sensitivity of our protocol, we analyzed three samples from patients after treatments expected to bear approximately 10% residual leukemic blasts, according to previous standard diagnostic analyses (Supporting Information Table S3). As shown in Figures 4C and 4D, we could detect aberrant blood composition in these samples and, importantly, the frequency of putative blasts, measured through WBD, was in good accordance with the previous diagnosis (12%, 8.2% and 15.7% on CD45+ cells in AML-5, AML-6, and ALL respectively). Finally, we had the opportunity to analyze the BM of a patient newly diagnosed with a low-differentiated Multiple Myeloma (MM). Interestingly, as shown in Figure 4E, we could detect a population of cells constituting 19.3% of total BM belonging to the fraction of unassigned events which usually represents on average only 0.2% of a normal BM sample (Fig. 3 and Supporting Information Fig. S3A). Strikingly by characterizing this population for the expression of all the other WBD markers we found that the 93,8% of these events were highly positive for the CD38 marker (Supporting Information Fig. S4E). This suggests that, through WBD, we most likely identified an accumulation of infiltrating plasmablasts (commonly identified as CD45^{mid} CD38^{high}) in the BM of this individual which accounted for 18,1% of the total CD45+ cells, (65).

DISCUSSION

As several human blood disorders are associated with an unbalanced distribution of hematopoietic cells in both PB and BM, the generation of tools for the analysis of the hematopoietic system composition remains one crucial goal to understand the causes of hematological diseases, to design novel therapeutic approaches and to test their efficacy. Over the past three decades, flow cytometry has been widely applied for

immune-phenotyping in clinical and research settings (1,2,29,30,47,65–70). A 17-multiparametric assay has been developed in the past for analyzing in details PB mature cells (68). However, this earlier protocol could not discriminate progenitor cells and therefore its application could not be extended to BM samples. Additionally, differently from the technique describe in this study, the previous assay could not benefit from the recent advancement in the fluorochromes design that makes our WBD protocol up-to-date with the most recent technology favoring its exploitation in the years to come. The low amount of blood required to achieve a comprehensive picture of the hematopoietic composition of a given sample makes WBD suitable for clinical screenings when limited amount of starting material is available. When tested on samples from Ad and Ped HD, WBD proved its sensitivity. Although we observed an overall similar cellular distribution among the different leukocyte compartments in Ped and Ad HD (Fig. 3B and Supporting Information Figs. S3A and S3B), we could detect the known subtle age-related differences in the hematopoietic composition, particularly related to the lymphoid immature B cell lineages (28.5% vs. 17.4% Pre-B cells on lymphocytes in Ped HD and in Ad HD respectively, Fig. 3B and Supporting Information Fig. S3D). This difference was found further accentuated in the very young individuals affected by MLD (Fig. 3D and Supporting Information Fig. S3D), where we found a higher content of immature B cells as compared to Ad HD (Supporting Information Figs. S3D and S3E). Thanks to the human-specific WBD design, one could envisage that this assay could be also exploited to comprehensively analyze the human-in-mouse graft in pre-clinical studies, fundamental for assessing the safety and efficacy of treatments and for studying the biology of human hematopoietic system (36,37,69–72).

In order to validate the WBD efficacy in detecting hematopoietic alterations in clinically relevant settings, we analyzed BM samples from ADA-SCID and WAS patients. We could show that WBD is capable not only of confirming the previously described hematopoietic alterations occurring in these individuals (4–7,9,10,17) but also of providing novel information on the hematopoietic landscape of these diseases. Indeed, together with the known defects in B cell contribution (Fig. 3C and Supporting Information Figs. S3D and S3E Table 2), we could observe alterations in HSPC compartment, supporting the notion that the functional

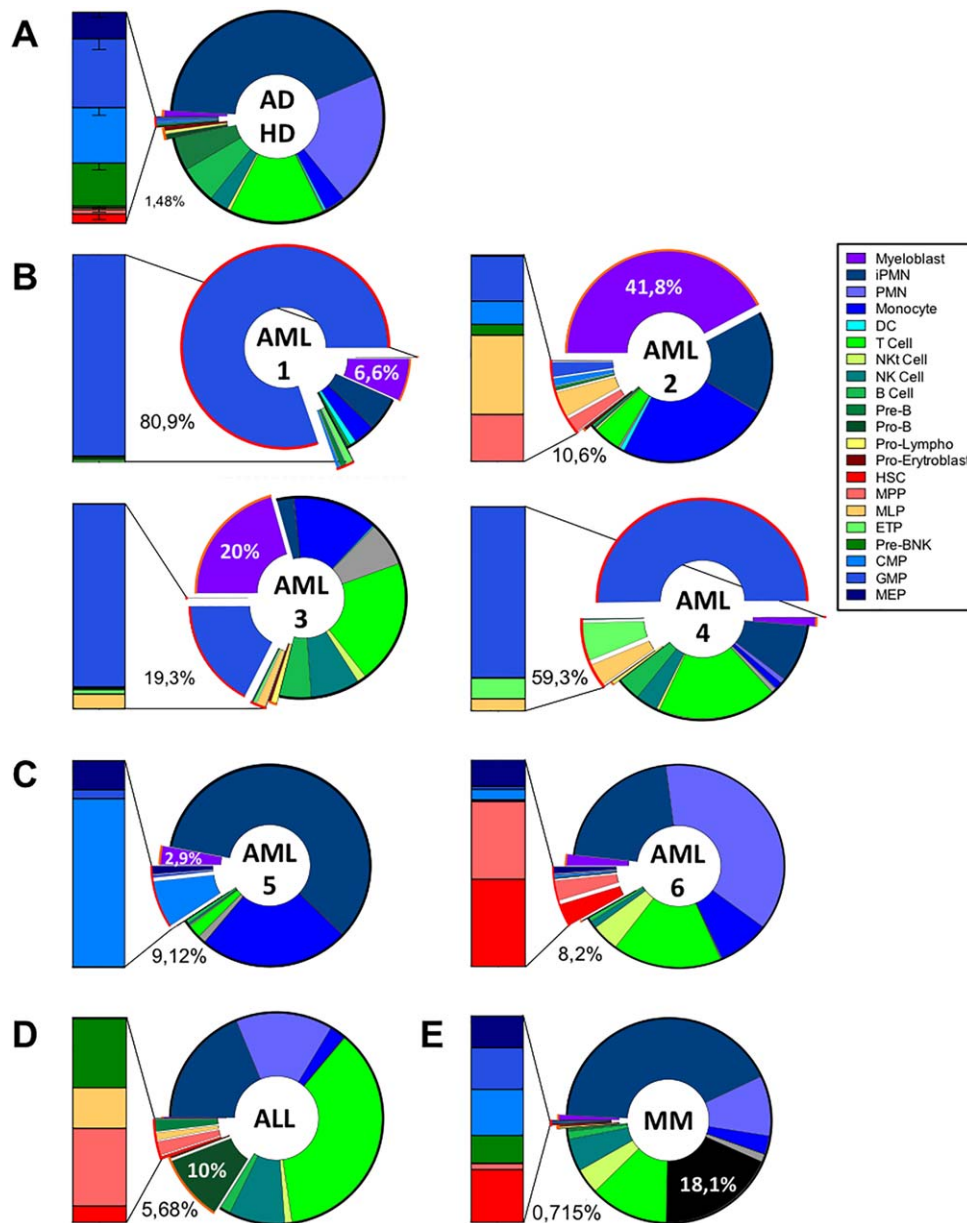


Figure 4. WBD analyses of BM samples from patients with myeloid or lymphoid leukemia. From **A** to **E**: WBD graphical representation showing BM composition in 1 representative adult HD (**A**), 6 patients with acute myeloid leukemia (AML) (**B** and **C**), 1 patient with acute lymphoid leukemia (ALL) (**D**) and 1 patient with multiple myeloma (MM) (**E**). The percentages indicate the relative frequency of the cells with immature markers likely belonging to leukemic blasts on total CD45+ cells. For the MM sample, we highlighted in black the fraction of CD38^{high} putative plasmablasts belonging to an elsewhere undefined compartment. [Color figure can be viewed at wileyonlinelibrary.com]

impairment causative of these PID also affects the very primitive stem-cell compartment (Supporting Information Fig. S3G and Table 2). Although these findings need to be further confirmed on a larger cohort of PID patients, they already support the use of WBD technology as a screening tool for the first characterization of immunodeficiencies, directing the choice of additional assays on specific cellular compartments. In this regard, WBD could also provide a relevant instrument for the evaluation of the BM composition of donor grafts prior to infusion and could be applied for the characterization of other cell sources enriched of HSPC,

including PB upon administration of mobilizing agents (38,39). Additionally, our protocol is suitable for the clinical monitoring of PID patients after allogeneic transplantation or GT to evaluate, at the same time, the level of re-establishment of mature blood cells and the long-term maintenance of all HSPC populations and for studying the dynamics of the hematopoietic reconstitution (73).

As a proof of principle of the qualitative evaluation of WBD potential, we tested our technology on samples from leukemic patients, both at diagnosis/relapse and after treatments (Supporting Information Table S3). Through WBD we

could clearly identify the blast populations and categorize the types of leukemia even on the samples with expected low blast content. Indeed, we found that the four acute leukemia samples displayed a highly skewed repertoire with respect to HD and a clear myeloid phenotype (Fig. 4B and Supporting Information Fig. S4B). On the other hand, in the samples analyzed after chemotherapy, we could identify residual myeloid and lymphoid leukemic blasts and evaluate their contribution, which was to levels comparable to the estimations made through the standard diagnostic assays based on multiple staining procedures (Figs. 4C and 4D, Supporting Information Table S3). Moreover, WBD was able to detect the presence of a large fraction of previously unidentified cells with “plasmablast-like” phenotype in the MM BM sample (Fig. 4E and Supporting Information Fig. S4E), suggesting that WBD technology is capable to provide a first categorization of the BM of leukemic patients that could guide investigators toward more detailed down-stream analyses. Importantly, the presence of antibodies specific for the HSPC subtypes represents a substantial advantage of WBD over the standard phenotypic characterizations allowing identifying with higher precision the level of maturation of the leukemic blasts. Indeed, through WBD we could unveil that AML-1 and AML-4 displayed a more immature phenotype with respect to AML-2 and AML-3 (Fig. 4B and Supporting Information Fig. S4B). Thus, this technology can provide in less than 2 hours important and timely readouts for directing therapeutic strategies on hospitalized individuals. Of note, by analyzing the phenotype of the residual blasts in two different AML patients (AML-5 and AML-6, Fig. 4) after chemotherapy, we could observe a diverse degree of differentiation of chemo-resistant blasts, with AML-5 displaying a “CMP-like” phenotype, while AML-6 showing a “HSC/MPP-like” phenotype. One could speculate that WBD may provide a tool for the detection of Leukemic stem cells (LSC) which represent a subset of AML cells showing an early stem/progenitor phenotype with the potential of preserving the leukemic population and generate relapses after treatment (74–76). In this regard, the actual sensitivity of WBD remains to be assessed on a wider cohort of patients with different types and degrees of leukemia. The capability of WBD on detecting residual clones in patients who underwent chemotherapy or BMT suggests that this technique could be also potentially exploited for the monitoring of MRD (11,12,26). MRD tracking is currently performed by assessing the so-called Leukemia Associated Aberrant Immunophenotype at diagnosis and monitoring it during the patient follow-up after treatments (50,53,77), but a major disadvantage of this approach is the current lack of uniformity on performing this assay among centers (50). Once implemented, the standardized and reproducible nature of WBD could overt these intrinsic constraints providing a common platform to reduce at minimum interlaboratory variability. Overall, we believe that the WBD protocol, allowing the simultaneous analysis of 23 different cell types including all the major mature lineage compartments, progenitors at different stages of maturation and rare subsets of HSPC, constitute a novel relevant tool for the analysis of PB and BM samples. The WBD has substantial

advantages on the analysis of HSPC compartment with respect to current technologies based on CD34+ isolation and purification, which might introduce analytical biases and negatively affect the cell yield. The possibility through WBD to analyze at the same time HSPC and mature cells starting from very small amounts of BM or PB allows studying the composition of human hematopoietic progenitors in different experimental settings like at steady-state hematopoiesis or upon stressed conditions, such as the ones related to hematopoietic defects, hematological tumors, pharmacological therapies, bone marrow transplantations, and gene therapy. Importantly, WBD could represent a useful tool for preclinical studies involving the use of humanized animal models where investigators might aim at analyzing small changes in BM and PB human blood cell composition upon treatment. In conclusion, WBD allows unambiguously identifying >99% of the cell subpopulations composing a blood sample in a reproducible, standardized, cost- and time-efficient manner. This technology represents a powerful tool for the analysis of human hematopoiesis with a wide spectrum of potential preclinical and clinical applications.

ACKNOWLEDGMENTS

The authors are grateful to the FRACTAL staff, in particular to Chiara Villa, Emanuele Canonico, and Monica Romanò for cell sorting and technical help for the instrumentations, SR-TIGET clinical trial office (TCTO) for clinical trial management and the physicians and nurses from the San Raffaele Pediatric Immuno-hematology and Stem Cell Programme Unit for patients' care. We thank the Cytometry Laboratory Unit for technical help in the set up of the morphology assay and Cristina Tresoldi for providing leukemic patients' samples from the San Raffaele Bio-bank.

AUTHOR CONTRIBUTIONS

L.B.R. designed and performed technical validations of the WBD protocol, analyzed the experiments, interpreted data and wrote the manuscript; S.S. performed technical validations of the WBD protocol, analyzed and interpreted data and wrote the manuscript; R.M. performed morphological evaluation in blind tests and characterize leukemic patients' samples; M.M., A.R. and M.E.B. provided clinical samples and patients' data; F.C. provided clinical samples and revised and interpreted the data; AA supervised research, interpreted data, revised the manuscript and participated as co-PI of the study; L.B. supervised research, interpreted data, wrote the manuscript and participated as co-PI of the study. All authors reviewed and approved the manuscript.

LITERATURE CITED

1. van Lochem EG, van der Velden VHJ, Wind HK, te Marvelde JG, Westerdal NAC, van Dongen JJM. Immunophenotypic differentiation patterns of normal hematopoiesis in human bone marrow: Reference patterns for age-related changes and disease-induced shifts. *Cytometry Part B Clin Cytom* 2004;60B:1–13.
2. Craig FE, Foon KA. Flow cytometric immunophenotyping for hematologic neoplasms. *Blood* 2008;111:3941–3967.
3. Cham B, Bonilla MA, Winkelstein J. Neutropenia associated with primary immunodeficiency syndromes. *Semin Hematol* 2002;39:107–112.

4. Apasov SG, Blackburn MR, Kellems RE, Smith PT, Sitkovsky MV. Adenosine deaminase deficiency increases thymic apoptosis and causes defective T cell receptor signaling. *J Clin Invest* 2001;108:131–141.
5. Sauer AV, Morbach H, Brigida I, Ng Y, Aiuti A, Meffre E. Defective B cell tolerance in adenosine deaminase deficiency is corrected by gene therapy. *J Clin Invest* 2012;122:2141–2152.
6. Brigida I, Sauer AV, Ferrua F, Giannelli S, Scaramuzza S, Pistoia V, Castiello MC, Barendregt BH, Cicalese MP, Casiraghi M, et al. B-cell development and functions and therapeutic options in adenosine deaminase – deficient patients. *J Allergy Clin Immunol* 2014;133:799–806.
7. Simon KL, Anderson SM, Garabedian EK, Moratto D, Sokolic RA, Candotti F. Molecular and phenotypic abnormalities of B lymphocytes in patients with Wiskott-Aldrich syndrome. *J Allergy Clin Immunol* 2014;133:896–899.e4.
8. Ochs HD, Slichter SJ, Harker LA, Von Behrens WE, Clark RA, Wedgwood RJ. The Wiskott-Aldrich syndrome: Studies of lymphocytes, granulocytes, and platelets. *Blood* 1980;55:243–252.
9. Park JY, Kob M, Prodeus AP, Rosen FS, Shcherbina A, Remold-O'Donnell E. Early deficit of lymphocytes in Wiskott-Aldrich syndrome: Possible role of WASP in human lymphocyte maturation. *Clin Exp Immunol* 2004;136:104–110.
10. Massa MJ, Ramesh N, Geha RS. Wiskott-Aldrich syndrome: A comprehensive review. *Ann NY Acad Sci* 2013;1285:26–43.
11. De Kouchkovsky I, Abdul-Hay M. Acute myeloid leukemia: A comprehensive review and 2016 update. *Blood Cancer J* 2016;e441:1–10.
12. Jabbour E, O'Brien S, Konopleva M, Kantarjian H. New insights into the pathophysiology and therapy of adult acute lymphoblastic leukemia. *Cancer* 2015;2517–2528.
13. Hunger SP, Mullighan CG. Acute lymphoblastic leukemia in children. *N Engl J Med* 2015;373:1541–1552.
14. Cunningham-Rundles C. Hematologic complications of primary immune deficiencies. *Blood Rev* 2002;16:61–64.
15. Morimoto Y, Routes JM. Immunodeficiency overview. *Prim Care - Clin Off Pract* 2008;35:159–173.
16. Booth C, Gaspar H. Pegademase bovine (PEG-ADA) for the treatment of infants and children with severe combined immunodeficiency (SCID). *Biol Targets Ther* 2009;3:349–358.
17. Castiello MC, Bosticardo M, Pala F, Catucci M, Chamberlain N, Van Zelm MC, Driessen GJ, Pac M, Bernatowska E, Scaramuzza S, et al. Wiskott-Aldrich Syndrome protein deficiency perturbs the homeostasis of B-cell compartment in humans. *J Autoimmun* 2014;50:42–50.
18. Grunebaum E, Mazzolari E, Porta F, Dallera D, Atkinson A, Reid B, Notarangelo LD, Roifman CM. Bone marrow transplantation for severe combined immune deficiency. *JAMA* 2006;295:508–518.
19. Neven B, Leroy S, Decaluwe H, Le Deist F, Picard C, Moshov D, Mahlaoui N, Debré M, Casanova J, Dal Cortivo L, et al. Long-term outcome after hematopoietic stem cell transplantation of a single-center cohort of 90 patients with severe combined immunodeficiency. *Blood* 2009;113:4114–4124.
20. Gaspar HB, Aiuti A, Porta F, Candotti F, Hershfield MS, Notarangelo LD. How I treat ADA deficiency. *Blood* 2009;114:3524–3532.
21. Hacein-Bey-Abina S, Hauer J, Lim A, Picard C, Wang GP, Berry CC, Martinache C, Rieux-Laucat F, Latour S, Belohradsky BH, et al. Efficacy of gene therapy for X-linked severe combined immunodeficiency. *N Engl J Med* 2010;363:355–364.
22. Fischer A, Hacein-Bey-Abina S, Cavazzana-Calvo M. Gene therapy of primary T cell immunodeficiencies. *Gene* 2013;525:170–173.
23. Kaufmann KB, Büning H, Galy A, Schambach A, Grez M. Gene therapy on the move. *EMBO Mol Med* 2013;5:1642–1661.
24. Cicalese MP, Aiuti A. Clinical applications of gene therapy for primary immunodeficiencies. *Hum Gene Ther* 2015;26:210–219.
25. Cicalese MP, Ferrua F, Castagnaro L, Pajno R, Barzagli F, Giannelli S, Dionisio F, Brigida I, Bonopane M, Casiraghi M, et al. Update on the safety and efficacy of retroviral gene therapy for immunodeficiency due to adenosine deaminase deficiency. *Blood* 2016;128:45–55.
26. Bhojwani D, Yang JJ, Pui C-H. Biology of childhood acute lymphoblastic leukemia. *Pediatr Clin North Am* 2015;62:47–60.
27. Oliveira E, Bacelar TS, Ciudad J, Ribeiro MCM, Garcia DRN, Sedek L, Maia SF, Aranha DB, Machado IC, Ikeda A, et al. Altered neutrophil immunophenotypes in childhood B-cell precursor acute lymphoblastic leukemia. *Oncotarget* 2016;7:24664–24676.
28. O'Donnell MR, Abboud CN, Altman J, Appelbaum FR, Arber DA, Attar E, Borate U, Coutre SE, Damon LE, Goorha S, et al. NCCN clinical practice guidelines acute myeloid leukemia. *J Natl Compr Canc Netw* 2012;10:984–1021.
29. Porwit A, Rajab A. Flow cytometry immunophenotyping in integrated diagnostics of patients with newly diagnosed cytopenia: One tube 10-color 14-antibody screening panel and 3-tube extensive panel for detection of MDS-related features. *Int J Lab Hematol* 2015;37:133–143.
30. Rajab A, Porwit A. Screening bone marrow samples for abnormal lymphoid populations and myelodysplasia-related features with one 10-color 14-antibody screening tube. *Cytometry B Clin Cytom* 2015;88B:253–260.
31. Piemontese S, Ciceri F, Labopin M, Bacigalupo A, Huang H, Santarone S, Gorin N-C, Koc Y, Wu D, Beelen D, et al. A survey on unmanipulated haploidentical hematopoietic stem cell transplantation in adults with acute leukemia. *Leukemia* 2015;29:1069–1075.
32. Warlick ED, Peffault De Latour R, Shanley R, Robin M, Bejanyan N, Xhaard A, Brunstein C, Sicre De Fontbrune F, Ustun C, Weisdorf DJ, et al. Biology of blood and marrow transplantation allogeneic hematopoietic cell transplantation outcomes in acute myeloid leukemia: Similar outcomes regardless of donor type. *Biol Blood Marrow Transplant* 2015;21:357–363.
33. Tsigotou P, Byrne M, Schmid C, Baron F, Ciceri F, Esteve J, Gorin NC, Giebel S, Mohty M, Savani BN, et al. Relapse of AML after hematopoietic stem cell transplantation: Methods of monitoring and preventive strategies. A review from the ALWP of the EBMT. *Bone Marrow Transplant* 2016;51:1–8.
34. Doulatov S, Notta F, Laurenti E, Dick JE. Hematopoiesis: A human perspective. *Cell Stem Cell* 2012;10:120–136.
35. Laurenti E, Dick JE. Molecular and functional characterization of early human hematopoiesis. *Ann N Y Acad Sci* 2012;1266:68–71.
36. Notta F, Doulatov S, Laurenti E, Poepl A, Jurisica I, Dick JE. Isolation of single human hematopoietic stem cells capable of long-term multilineage engraftment. *Science* 2011;333:218–221.
37. Doulatov S, Notta F, Eppert K, Nguyen LT, Ohashi PS, Dick JE. Revised map of the human progenitor hierarchy shows the origin of macrophages and dendritic cells in early lymphoid development. *Nat Immunol* 2010;11:585–593.
38. Bozdogan SC, Tekgunduz E, Altuntas F. The current status in hematopoietic stem cell mobilization. *J Clin Apheresis* 2015;30:273–280.
39. Cimato TR, Furlage RL, Conway A, Wallace PK. Simultaneous measurement of human hematopoietic stem and progenitor cells in blood using multicolor flow cytometry. *Cytometry B Clin Cytom* 2016;90B:415–423.
40. Wright DE, Wagers AJ, Gulati AP, Johnson FL, Weissman IL. Physiological migration of hematopoietic stem and progenitor cells. *Science* 2001;294:1933–1936.
41. Eidenschink L, Dizerega G, Rodgers K, Bartlett M, Wells DA, Loken MR. Basal levels of CD34 positive cells in peripheral blood differ between individuals and are stable for 18 months. *Cytometry B Clin Cytom* 2012;82B:18–25.
42. Mazo IB, Massberg S, von Andrian UH. Hematopoietic stem and progenitor cell trafficking. *Trends Immunol* 2011;32:493–503.
43. Fuchigami K, Mori H, Matsuo T, Iwanaga M, Nagai K, Kuriyama K, Tomonaga M. Absolute number of circulating CD34+ cells is abnormally low in refractory anemias and extremely high in RAEB and RAEB-t; novel pathologic features of myelodysplastic syndromes identified by highly sensitive flow cytometry. *Leuk Res* 1999;24:163–174.
44. Kikuchi-Taura A, Soma T, Matsuyama T, Stern DM, Taguchi A. A new protocol for quantifying CD34+ Cells. *Texas Hear. Inst. J* 2006;33:427–429.
45. Cohen KS, Cheng S, Larson MG, Cupples LA, McCabe EL, Wang YA, Ngwa JS, Martin RP, Klein RJ, Hashmi B, et al. Circulating CD34+ progenitor cell frequency is associated with clinical and genetic factors. *Blood* 2013;121:e50–e57.
46. Napolitano M, Gerardi C, Lucia A, Di Accardo PA, Rizzuto L, Ferraro M, Siragusa S, Buscemi F. Hematopoietic peripheral circulating blood stem cells as an independent marker of good transfusion management in patients with b-thalassemia: Results from a preliminary study. *Transfusion* 2016;56:3–6.
47. Jacob M-C, Souvignet A, Pont J, Solly F, Mondet J, Kesr S, Pernollet M, Dumestre-Perard C, Campos L, Cesbron J-Y. One tube with eight antibodies for 14-part bone marrow leukocyte differential using flow cytometry. *Cytometry B Clin Cytom* 2016;90B:1–11.
48. O'Donnell E, Ernst DN, Hingorani R. Multiparameter flow cytometry: Advances in high resolution analysis. *Immune Netw* 2013;13:43–54.
49. Schwonzen M, Diehl V, Dellanna M, Staib P. Immunophenotyping of surface antigens in acute myeloid leukemia by flow cytometry after red blood cell lysis. *Leuk Res* 2007;31:113–116.
50. Chatterjee BT, Mallhi SCRS, Venkatesan LCS. Minimal residual disease detection using flow cytometry: Applications in acute leukemia. *Med J Armed Forces India* 2016;72:152–156.
51. Van De Geijn G, Van Rees V, Van Pul-bom N, Birnie E, Janssen H, Pegels H, Beunis M, Njo T. LeukoFlow: Multiparameter extended white blood cell differentiation for routine analysis by flow cytometry. *Cytometry Part A* 2011;79A:694–706.
52. Basso G, Buldini B, De Zen L, Orfao A. New methodologic approaches for immunophenotyping acute leukemias. *Hematologica* 2001;86:675–692.
53. Karawajew L, Dworzak M, Ratei R, Rhein P, Gaipa G, Buldini B, Basso G, Hrusak O, Ludwig W-D, Henze G, et al. Minimal residual disease analysis by eight-color flow cytometry in relapsed childhood acute lymphoblastic leukemia. *Haematologica* 2015;100:935–944.
54. Notta F, Zandi SS, Takayama N, Dobson S, Gan OI, Wilson G, Kaufmann KB, McLeod J, Laurenti E, Dunant CF, et al. Distinct routes of lineage development reshape the human blood hierarchy across ontogeny. *Science* 2016;351: aab2116.1–9.
55. Ornatsky O, Bandura D, Baranov V, Nitz M, Winnik MA, Tanner S. Highly multiparametric analysis by mass cytometry. *J Immunol Methods* 2010;361: 1–20.
56. Nicholas KJ, Greenplate AR, Flaherty DK, Matlock BK, Juan JS, Smith RM, Irish JM, Kalam SA. Multiparameter analysis of stimulated human peripheral blood mononuclear cells: A comparison of mass and fluorescence cytometry. *Cytometry Part A* 2016;89A:271–280.
57. Wood B. Multicolor immunophenotyping: Human immune system hematopoiesis. *Methods Cell Biol* 2004;75:559–576.
58. Cerwenka A, Lanier LL. Natural killer cell memory in infection, inflammation and cancer. *Nat Publ Gr* 2016;16:112–123.
59. Godfrey DI, Uldrich AP, McCluskey J, Rossjohn J, Moody DB. The burgeoning family of unconventional T cells. *Nat Immunol* 2015;16:1114–1123.
60. Jin H, Kim H-S, Kim S, Kim HO. Erythropoietic potential of CD34+ hematopoietic stem cells from human cord blood and G-CSF-mobilized peripheral blood. *Biomed Res Int* 2014;2014:1–9.
61. Perfetto SP, Ambrozak D, Nguyen R, Chattopadhyay P, Roederer M. Quality assurance for polychromatic flow cytometry. *Nat Protoc* 2006;1:1522–1530.

62. Giblett ER, Anderson JE, Cohen F, Pollara B, Meuwissen HJ. Adenosine-deaminase deficiency in two patients with severely impaired cellular immunity. *Lancet* 1972; 300:1067–1069.
63. van Rappard DF, Boelens JJ, Wolf NI. Metachromatic leukodystrophy: Disease spectrum and approaches for treatment. *Best Pract Res Clin Endocrinol Metab* 2015;29: 261–273.
64. Sessa M, Lorioli L, Fumagalli F, Acquati S, Redaelli D, Baldoli C, Canale S, Lopez ID, Morena F, Calabria A, et al. Lentiviral haemopoietic stem-cell gene therapy in early-onset metachromatic leukodystrophy: An ad-hoc analysis of a non-randomised, open-label, phase 1/2 trial. *Lancet* 2016;6736:1–12.
65. Kalina T, Flores-Montero J, van der Velden VHJ, Martin-Ayuso M, Böttcher S, Ritgen M, Almeida J, Lhermitte L, Asnafi V, Mendonça A, et al. EuroFlow standardization of flow cytometer instrument settings and immunophenotyping protocols. *Leukemia* 2012;26:1986–2010.
66. Luria D, Rosenthal E, Steinberg D, Kodman Y, Safanaiev M, Amariglio N, Avigad S, Stark B, Izraeli S. Prospective comparison of two flow cytometry methodologies for monitoring minimal residual disease in a multicenter treatment protocol of childhood acute lymphoblastic leukemia. *Cytometry Part B Clin Cytom* 2010;78B: 365–371.
67. Hasan M, Beitz B, Rouilly V, Libri V, Urrutia A, Duffy D, Cassard L, Di Santo JP, Mottez E, Quintana-Murci L, et al. Semi-automated and standardized cytometric procedures for multi-panel and multi-parametric whole blood immunophenotyping. *Clin Immunol* 2015;157:261–276.
68. Perfetto SP, Chattopadhyay PK, Roederer M. Seventeen-colour flow cytometry: Unravelling the immune system. *Nat Rev Immunol* 2004;4:648–655.
69. Goyama S, Wunderlich M, Mulloy JC. Xenograft models for normal and malignant stem cells. *Blood* 2015;125:2630–2641.
70. Naldini L. Ex vivo gene transfer and correction for cell-based therapies. *Nat Rev Genet* 2011;12:301–315.
71. Genovese P, Schirotti G, Escobar G, Di Tomaso T, Firrito C, Calabria A, Moi D, Mazzieri R, Bonini C, Holmes MC, et al. Targeted genome editing in human repopulating haematopoietic stem cells. *Nature* 2014;510:235–240.
72. Arber C, Brenner MK, Reddy P. Mouse models in bone marrow transplantation and adoptive cellular therapy. *Semin Hematol* 2013;50:131–144.
73. Biasco L, Pellin D, Scala S, Dionisio F, Basso-Ricci L, Leonardelli L, Scaramuzza S, Baricordi C, Ferrua F, Cicalese MP, et al. In vivo tracking of human hematopoiesis reveals patterns of clonal dynamics during early and steady-state reconstitution phases. *Cell Stem Cell* 2016;19:107–119.
74. Guzman ML, Allan JN. Concise review: Leukemia stem cells in personalized medicine. *Stem Cells* 2014;32:844–851.
75. Wiseman DH, Greystoke BF, Somerville TCP. The variety of leukemic stem cells in myeloid malignancy. *Oncogene* 2014;33:3091–3098.
76. Jamieson CHM, Ailles LE, Dyalla SJ, Muijtjens M, Jones C, Zehnder JL, Gotlib J, Li K, Manz MG, Keating A, et al. Granulocyte-macrophage progenitors as candidate leukemic stem cells in blast-crisis CML. *N Engl J Med* 2004; 351:657–667.
77. Olaru D, Campos L, Flandrin P, Nadal N, Duval A, Chautard S, Guyotat D. Multi-parametric analysis of normal and postchemotherapy bone marrow: Implication for the detection of leukemia-associated immunophenotypes. *Cytometry B Clin Cytom* 2008;74B:17–24.